Chinese Journal of Electronics
vol. 33, no. 1, pp. 175–184, January 2024
https://doi.org/10.23919/cje.2022.00.112

RESEARCH ARTICLE

Rapid Phase Ambiguity Elimination Methods for DOA Estimator via Hybrid Massive MIMO Receive Array

Xichao ZHAN[1], Zhongwen SUN[1], Feng SHU[1,2], Yiwen CHEN[1], Xin CHENG[2], Yuanyuan WU[1], Qi ZHANG[1], Yifan LI[2], and Peng ZHANG[1]

1. *School of Information and Communication Engineering, Hainan University, Haikou 570228, China*
2. *School of Electronic and Optical Engineering, Nanjing University of Science and Technology, Nanjing 210094, China*

Corresponding author: Feng SHU, Email: shufeng0101@163.com
Manuscript Received May 6, 2022; Accepted August 29, 2022

Abstract — For a sub-connected hybrid multiple-input multiple-output (MIMO) receiver with K subarrays and N antennas, there exists a challenging problem of how to rapidly remove phase ambiguity in only single time-slot. A direction of arrival (DOA) estimator of maximizing received power (Max-RP) is proposed to find the maximum value of K-subarray output powers, where each subarray is in charge of one sector, and the center angle of the sector corresponding to the maximum output is the estimated true DOA. To make an enhancement on precision, Max-RP plus quadratic interpolation (Max-RP-QI) method is designed. In the proposed Max-RP-QI, a quadratic interpolation scheme is adopted to interpolate the three DOA values corresponding to the largest three receive powers of Max-RP. To achieve the Cramer Rao lower bound, a Root-MUSIC plus Max-RP-QI scheme is developed. Simulation results show that the proposed three methods eliminate the phase ambiguity during one time-slot and also show low computational complexities. The proposed Root-MUSIC plus Max-RP-QI scheme can reach the Cramer Rao lower bound, and the proposed Max-RP and Max-RP-QI are still some performance losses 2–4 dB compared to the Cramer Rao lower bound.

Keywords — Hybrid analog and digital, Direction of arrival, Massive hybrid multiple-input multiple-output, Phase ambiguity, Low computational complexity.

Citation — Xichao ZHAN, Zhongwen SUN, Feng SHU, *et al.*, "Rapid Phase Ambiguity Elimination Methods for DOA Estimator via Hybrid Massive MIMO Receive Array," *Chinese Journal of Electronics*, vol. 33, no. 1, pp. 175–184, 2024. doi: 10.23919/cje.2022.00.112.

I. Introduction

Due to the development of computing processors and digital signal processing technology, array signal processing (ASP), particularly large-scale ASP, has attracted more and more attention. As one of key techniques of ASP [1], [2], direction of arrival (DOA) estimation has been widely used in fifth generation mobile communication (5G) [3], [4], direction modulation network [5], [6], radar, sonar, earthquake monitoring, aerospace, mmWave communications [7], [8], unmanned aerial vehicle (UAV) communications [9], [10], satellite communications, and angle of arrival (AOA) positioning [11], [12].

It is critical to infer the presence or absence of an emitter before performing DOA measurements. If there exists no emitter, then it is obvious that no DOA estimation operation is required. In [13], two signal detectors using the generalized likelihood ratio test (GLRT) paradigm based on sample covariance matrices were proposed. However, the computational complexity will increase significantly with the number of the antenna tends to large-scale. And in [14], the three high-performance detectors defined on egien-space of sample covariance were proposed to achieve much better performance than conventional GLRT and enegergy detection in terms of receiver operation curves (ROC). Regrettably, it has a good accuracy only when detecting a single emitter. To improve the detection accuracy, the multi-layer neural

Guest Editor: Prof. Junhui ZHAO, East China Jiaotong University.

networks (ML-NN) was introduced in [15] for inferring the number of passive emitters. Compared with the traditional signal detectors and classic information theoretic criteria like AIC and MDL, the ML-NN used the features extracted from the received signals for classification, and the final accuracy of inferring the number of signals reached more than 70%.

Recently, as the massive multiple-input multiple-output (MIMO) attracts widespread academic interests, the DOA estimation using receive massive MIMO array emerges. However, the massive fully-digital MIMO receive array structure requires a large numbers of analog-to-digital converters (ADCs) and RF links, which leads to a high circuit cost. In [16], a generalized sparse Bayesian learning algorithm is integrated into the 1-bit DOA estimation. In [17], a new receive array framework with low-resolution ADCs was designed, and a closed-form expression of Cramer Rao lower bound (CRLB) was derived to evaluate the performance loss. From analysis, it is found that 2–3 bits ADC is sufficient to achieve a trivial performance loss. And, in [18], the authors had made an investigation on the performance loss of DOA estimation under hybrid ADCs structure and show that low-resolution ADCs with only a few bits (up to 4 bits) can achieve an acceptable performance loss for DOA measurement.

Due to the fact the massive hybrid analog and digital (HAD) MIMO [19]–[24] owns three important properties: low circuit loss, low computational complexity, and high-spatial-angle-resolution, DOA estimation based massive HAD MIMO receiver has attracted a large amount of research activities. In [20], three low-complexity and high-precision methods were developed to achieve the CRLB of HAD, but still require $M+1$ time-slots to eliminate the inherent deficiency of phase ambiguity, where M is the number of antennas per sub-array. As M increase, the DOA measurement delay will grow linearly. In order to reduce the estimate time delay, a fast phase ambiguity elimination method of finding the true emitter direction using only two time-slots was proposed in [23]. In [25], a two-layer HAD (TLHAD) structure was constructed, which can eliminate phase ambiguity with a single time-slot, which dramatically decreases the DOA measurement delay. Aiming at phase ambiguity of DOA estimation in large-scale HAD MIMO systems, in [26], an extended discrete fourier transform (DFT) algorithm is proposed, which combines the DFT method with non-circular (NC) signal and achieves DOA estimation using a single snapshot. Furthermore, in [27], a low-complexity deep-learning method for hybrid HAD MIMO receiver using uniform circular arrays was proposed to learn the function of mapping the receiving signal vector into DOA. Subsequently, a machine-learning (ML) framework using the probability density function (PDF) is proposed to improve the precision of measuring DOA in [28]. However, many samples and much time are required in the training process of the network.

As previously summarized, the TLHAD structure has reduced M time-slots in [20] and 1 time-slot in [23] to single one, which significantly improve the speed of DOA measurement. But this structure is made up of two distinct parts: fully-digital and hybrid sub-connected, which increase the complexity of designing RF circuit and leads to an increasing circuit cost. In this paper, only a pure sub-connected hybrid structure is used to achieve a single-time-slot fast DOA estimator. This will make an effective complexity and cost reduction. Our main contributions are summarized as follows:

1) To rapidly eliminate the phase ambiguity of direction finding in HAD structure, a method of maximizing received power (Max-RP) is proposed. Its basic idea is to divide the angle range $[0, 2\pi]$ into K sectors. At receiver, analog beamforming per subarray is conducted and is equal to the steering vector of its center angle of the corresponding sector. Finally, the sector center angle corresponding to the maximum value of all subarray outputs is just the true DOA. To further improve the estimate precision, a new methods is developed. The method is actually a quadratic interpolation using the three largest DOA values of Max-RP to improve its performance, called Max-RP-QI. In accordance with simulation results, the proposed two methods with approximately identical computational complexities have a descending order in performance: Max-RP-QI and Max-RP.

2) To further enhance the estimate performance, a two-stage method is proposed as follows: generating a set of candidate solutions by Root-MUSIC and removing pseudo-solutions by Max-RP-QI, called Root-MUSIC plus Max-RP-QI. Simulation results show that the proposed Root-MUSIC plus Max-RP-QI estimator can achieve the CRLB and performs much better than the proposed Max-RP-QI, and Max-RP in the high SNR regions with slightly higher-computational-complexity than Max-RP.

The remainder of this paper is organized as follows. Section II describes the system model. In Section III, three estimators, Max-RP, Max-RP-QI and Root-MUSIC plus Max-RP-QI, are proposed to use only one time-slot to find the true direction angle of emitter at the cost of approximately 2–4 dB performance loss, and computational complexities are also analyzed. We present our simulation results in Section IV. Finally, we make our conclusions in Section V.

Notations: throughout this paper, boldface lower case and upper case letters represent vectors and matrices, respectively. Signs $(\cdot)^{\mathrm{T}}, (\cdot)^*, (\cdot)^{\mathrm{H}}, (\cdot)^{-1}$ and $\|\cdot\|$ denote the transpose operation, conjugate operation, conjugate transpose operation, inverse operation, and 2-norm operation, respectively. The notation $\boldsymbol{I}_M$ is the $M \times M$ identity matrix. The sign $\mathbb{E}\{\cdot\}$ represents the expectation operation, $\mathrm{diag}(\cdot)$ denotes the diagonal operator, $\arg(\cdot)$ means the argument of a complex number.

II. System Model

Figure 1 depicts the architecture of a HAD receiver

based on massive MIMO. The HAD antenna array receives a far-field narrowband signal $s(t)\mathrm{e}^{\mathrm{j}2\pi f_c t}$, where $s(t)$ is the narrowband signal, f_c is the carrier frequency, and uniform linear array (ULA) with N antennas. The ULA is divided into K subarrays with each subarry containing M antennas, where $N = KM$.

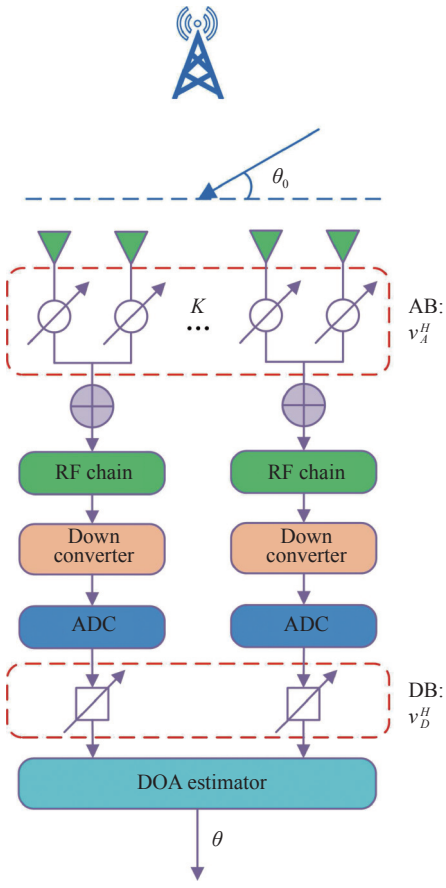

Figure 1 ULA hybrid beamforming sub-connected architecture. (AB: analog beamforming; DB: digital beamforming).

Considering sub-arrays are mutually independent of each other, the array manifold vector corresponding to subarray k can be expressed as

$$\boldsymbol{a}_k(\theta_0) = \mathrm{e}^{\mathrm{j}2\pi\psi_k(\theta_0)}\left[\mathrm{e}^{j2\pi\psi_k(1)}, \ldots, \mathrm{e}^{\mathrm{j}2\pi\psi_k(M)}\right]^{\mathrm{T}} \quad (1)$$

where $\psi_k(m)$ is the phase shift of signal at the baseband corresponding to the time delay from the source to antenna elements. And $\psi_{\theta_k}(m), m = 1, 2, \ldots, M$ is expressed as

$$\psi_k(\theta_0) = \frac{(k - 1 - K/2)Md\cos\theta_0}{\lambda} \quad (2)$$

and

$$\psi_k(m) = \frac{(m - \dfrac{M}{2})d\cos\theta_0}{\lambda},\ m = 1, 2, \ldots, M \quad (3)$$

where λ is the wavelength of the carrier frequency. d_m is the distance from a common reference point to the mth antenna. The analog beamforming (AB) vector corresponding to subarray k is designed as

$$\boldsymbol{v}_{A_k}(\theta_k) = \mathrm{e}^{\mathrm{j}2\pi\psi_k(\theta_0)}\boldsymbol{a}_k^{\mathrm{H}}(\theta_k) \quad (4)$$

such that phase alignment at subarray k is achieved.

In this paper, d is chosen to be half of the wavelength as usual (i.e., $d = \dfrac{\lambda}{2}$). After passing through parallel RF chain, down-conversion and ADC, the receive single M dimensional vector of subarray k from the emitter with direction angle being θ_0 can be expressed as follows:

$$\boldsymbol{y}_k(t) = \boldsymbol{v}_{A_k}H(\theta_k)\boldsymbol{a}(\theta_0)s(t) + \boldsymbol{w}_k(t),\ k = 1, 2, \ldots, K \quad (5)$$

where $\boldsymbol{w}_k(t) \sim \mathcal{CN}(0, \sigma_w^2\boldsymbol{I}_M)$ is the additive white Gaussian noise (AWGN) vector. similarly, $\phi_{\theta_0}(m) = \dfrac{d_m\cos\theta_0}{\lambda}$, $m = 1, 2, \ldots, M$. And via digital beamforming (DB) operation, the receive single vector becomes

$$\boldsymbol{r}_k(t) = \boldsymbol{v}_{D_k}^{\mathrm{H}}\boldsymbol{v}_{A_k}^{\mathrm{H}}(\theta_k)\boldsymbol{a}(\theta_0)s(t) + \boldsymbol{v}_{D_k}^{\mathrm{H}}\boldsymbol{w}_k(t) \quad (6)$$

where the DB vector is defined $\boldsymbol{v}_{D_k} = [\upsilon_1, \upsilon_2, \ldots, \upsilon_K]^{\mathrm{T}}$. For convenience below, the DB vector $\boldsymbol{v}_{D_k}$ is fixed to a vector of all ones, i.e., $\boldsymbol{v}_{D_k} = [1, 1, \ldots, 1]^{\mathrm{T}}$.

III. Proposed Three Fast DOA Estimators

In this section, to accelerate the elimination of phase ambiguity, the Max-RP method is first proposed, where the total angle range $[0, 2\pi]$ are equally partitioned into K sectors and each subarray takes charge of its owns sector. The center angle of the sector corresponding to the largest one among all subarray output powers is taken to be the final estimate DOA value. To improve the estimation accuracy, following Max-RP, a quadratic interpolation was performed by using the three largest RPs, called Max-RP-QI. To further enhance the estimate performance close to CRLB, the combining method of Root-MUSIC and Max-RP-QI was designed, and contains the following two steps: generating a set of candidate solutions by Root-MUSIC and removing pseudo-solutions by Max-RP-QI.

1. Proposed Max-RP

Figure 2 plots the block diagram of the Max-RP proposed by us. In this figure, each subarray is in charge of a sample angle range corresponding to one sector. The total angle range $[0, 2\pi]$ are divided into K subintervals. The output RP is viewed a function of discrete subarray index. Max-RP is eqvilent to find the maximum of this function.

From Figure 1 and equation (5), after AB, the output of subarray k is

$$y_k(t) = \gamma_k(\theta_k - \theta_0)s(t) + w_k(t),\ k = 1, 2, .., K \quad (7)$$

where

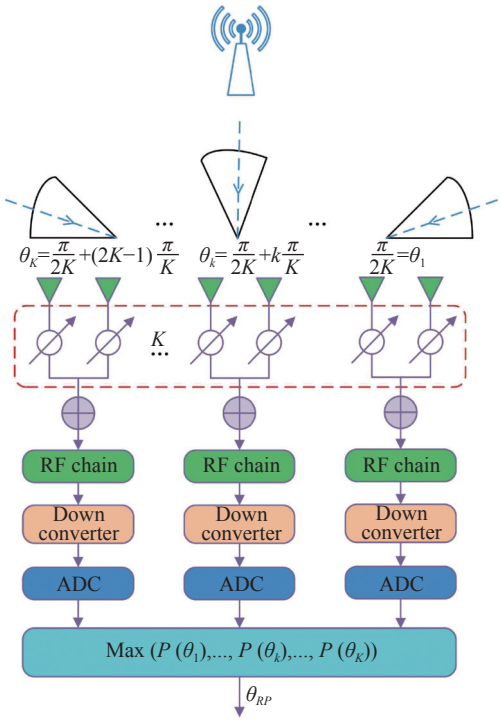

Figure 2 Proposed Max-RP structure.

$$\gamma_k(\theta_k-\theta_0)=\boldsymbol{v}_{A_k}^{\mathrm{H}}(\theta_k)\boldsymbol{a}(\theta_0)=\frac{\exp\left\{\mathrm{j}\frac{2\pi}{\lambda}Md(\cos\theta_0-\cos\theta_k)\right\}-1}{\exp\left\{\mathrm{j}\frac{2\pi}{\lambda}d(\cos\theta_0-\cos\theta_k)\right\}-1} \tag{8}$$

with θ_k belonging to

$$\Theta=\left\{\frac{\pi}{K},\frac{3\pi}{K},\ldots,\frac{(2K-1)\pi}{K}\right\} \tag{9}$$

It is assumed that the beamforming vector is known, the received signal power can be expressed as

$$\begin{aligned}&P(\theta_k)\\&=\mathbb{E}\left\{y_k(t)y_k(t)^{\mathrm{H}}\right\}\\&=\mathbb{E}\left\{\left[\gamma_k(\theta_k-\theta_0)s(t)+w_k(t)\right]\left[\gamma_k(\theta_k-\theta_0)s(t)+w_k(t)\right]^{\mathrm{H}}\right\}\end{aligned} \tag{10}$$

Since noise is independent and uncorrelated, we have

$$\begin{aligned}\mathbb{E}\left\{\gamma_k(\theta_k-\theta_0)s(t)w_k(t)^{\mathrm{H}}\right\}&=\gamma_k(\theta_k-\theta_0)\mathbb{E}\left\{s(t)w_k(t)^{\mathrm{H}}\right\}\\&=0\\\mathbb{E}\left\{w_k(t)\left[\gamma_k(\theta_k-\theta_0)s(t)\right]^{\mathrm{H}}\right\}&=\gamma_k(\theta_k-\theta_0)^*\mathbb{E}\left\{w_k(t)s(t)^{\mathrm{H}}\right\}\\&=0\end{aligned} \tag{11}$$

Substituting equation (11) into (10) yields

$$\begin{aligned}P(\theta_k)&=\mathbb{E}\left\{y_k(t)y_k(t)^{\mathrm{H}}\right\}\\&=\gamma_k(\theta_k-\theta_0)\mathbb{E}\left\{s(t)s(t)^{\mathrm{H}}\right\}\gamma_k(\theta_k-\theta_0)^*\\&\quad+\mathbb{E}\left\{w_k(t)w_k(t)^{\mathrm{H}}\right\}\end{aligned} \tag{12}$$

where $P_{s,k}=\mathbb{E}\{s(t)s(t)^{\mathrm{H}}\}$ and $\sigma_{w,k}^2=\mathbb{E}\{w_k(t)w_k(t)^{\mathrm{H}}\}$. Then, we have

$$P(\theta_k)=P_{s,k}+\sigma_{w,k}^2,k=1,2,\ldots,K \tag{13}$$

Actually, $P(\theta_k)$ cannot be obtained directly. However, it can be obtained from the available data and can be expressed as

$$\begin{aligned}&P(\theta_k)\\&=\frac{1}{L}\sum_{l=1}^{L}\left\{y_k(l)y_k(l)^{\mathrm{H}}\right\}\\&=\frac{1}{L}\sum_{l=1}^{L}\Big\{\left[\gamma_k(\theta_k-\theta_0)s(l)+w_k(l)\right]\\&\quad\cdot\left[\gamma_k(\theta_k-\theta_0)s(l)+w_k(l)\right]^{\mathrm{H}}\Big\}\\&=\frac{1}{L}\Big(\sum_{l=1}^{L}\left\{\left[\gamma_k(\theta_k-\theta_0)s(l)\right]\left[\gamma_k(\theta_k-\theta_0)s(l)\right]^{\mathrm{H}}\right\}\\&\quad+\sum_{l=1}^{L}\left\{\left[\gamma_k(\theta_k-\theta_0)s(l)\right]w_k(l)^{\mathrm{H}}\right.\\&\quad\left.+w_k(l)\left[\gamma_k(\theta_k-\theta_0)s(l)\right]^{\mathrm{H}}\right\}+\sum_{l=1}^{L}\left\{w_k(l)w_k(l)H\right\}\Big)\end{aligned} \tag{14}$$

Similarly, the noise is independent and uncorrelated, we have

$$\begin{aligned}&\sum_{l=1}^{L}\left\{\left[\gamma_k(\theta_k-\theta_0)s(l)\right]w_k(l)^{\mathrm{H}}+w_k(l)\left[\gamma_k(\theta_k-\theta_0)s(l)\right]^{\mathrm{H}}\right\}\\&=0\end{aligned} \tag{15}$$

It follows from the above that equation (14) is rewritten as

$$\begin{aligned}P(\theta_k)=&\frac{1}{L}\Big(\sum_{l=1}^{L}\left[\gamma_k(\theta_k-\theta_0)s(l)\right]\left[\gamma_k(\theta_k-\theta_0)s(l)\right]^{\mathrm{H}}\Big\}\\&+\sum_{l=1}^{L}\left\{w_k(l)w_k(l)^{\mathrm{H}}\right\}\Big)\end{aligned} \tag{16}$$

Let us defined $P_s=\frac{1}{L}\sum_{l=1}^{L}\{s(l)s(l)^{\mathrm{H}}\}$ and $\sigma_w^2=\frac{1}{L}\sum_{l=1}^{L}\{w_k(l)w_k(l)^{\mathrm{H}}\}$. Due to the $\gamma(\theta_k-\theta_0)$ is a scalar, so when L is sufficiently large, we have

$$\begin{aligned}&\frac{1}{L}\sum_{l=1}^{L}\left\{\left[\gamma_k(\theta_k-\theta_0)s(l)\right]\left[\gamma_k(\theta_k-\theta_0)s(l)\right]^{\mathrm{H}}\right\}\\&=P_s\gamma(\theta_k-\theta_0)\gamma(\theta_k-\theta_0)^*=P_s\gamma(\theta_k-\theta_0)^2\end{aligned} \tag{17}$$

It follows from the above that equation (16) is rewritten as

$$P(\theta_k)=P_s\gamma(\theta_k-\theta_0)^2+\sigma_w^2 \tag{18}$$

The received signal power of this receiver structure can therefore be expressed in the vector form as follows

$$\boldsymbol{P} = [P(\theta_1), P(\theta_2), \ldots, P(\theta_K)] \tag{19}$$

Eventually, the estimated direction angle is

$$\theta_{RP} = \arg \max_{\boldsymbol{\theta_k} \in \Theta} \boldsymbol{P}(\theta_k) \tag{20}$$

2. Proposed Max-RP-QI

In the preceding subsection, the Max-RP estimator is actually a global search with stepsize $2\pi/K$, and its resolution is $2\pi/K$. This will lead to a result that improving its precision require to increase the number of subarrays. To improve its estimate accuracy, following the maximizing operation, a quadratic interpolation is used over the three largest RPs in Figure 3. The new quadratic curve is maximized to find the more precise DOA.

From [29], a quadratic form is given as

$$f(\theta) = c + b\theta + a\theta^2 = P(\theta) \tag{21}$$

Taking the derivative of the above equation (21) with respect to θ equals zero, we have

$$\theta_{QI} = -\frac{b}{2a} \tag{22}$$

According to Figure 3, assuming that the received signal power achieves its maximum value in the kth sector, the system of linear equations of variables a, b and c is expressed as

$$\begin{cases} P(\theta_{k-1}) = c + b\theta_{k-1} + a\theta_{k-1}^2 \\ P(\theta_k) = c + b\theta_k + a\theta_k^2, \qquad (k = 1, 2, \ldots, K) \\ P(\theta_{k+1}) = c + b\theta_{k+1} + a\theta_{k+1}^2 \end{cases} \tag{23}$$

where $\theta_k = \theta_{RP}$ corresponds to the subarray or sector index of the maximum RP. The equation (23) is rewritten in the matrix-vector form

$$\begin{bmatrix} 1 & \theta_{k-1} & \theta_{k-1}^2 \\ 1 & \theta_k & \theta_k^2 \\ 1 & \theta_{k+1} & \theta_{k+1}^2 \end{bmatrix} \begin{bmatrix} c \\ b \\ a \end{bmatrix} = \begin{bmatrix} P(\theta_{k-1}) \\ P(\theta_k) \\ P(\theta_{k+1}) \end{bmatrix} \tag{24}$$

Then, let us define

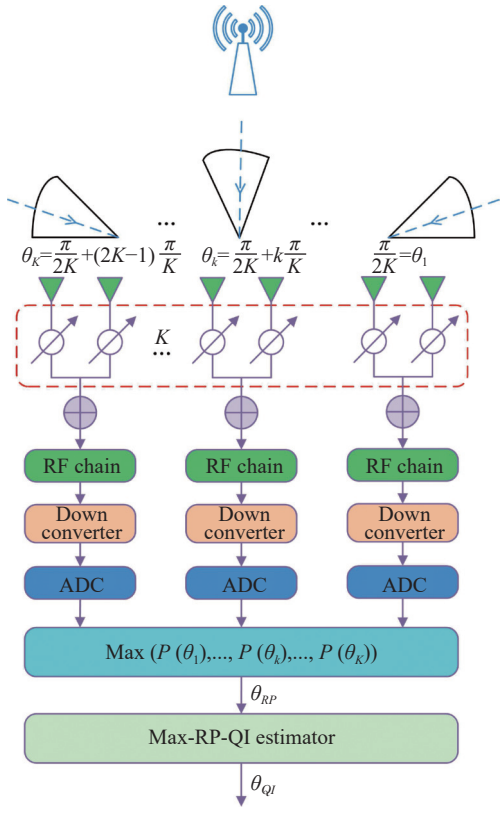

Figure 3 Proposed Max-RP-QI structure.

$$\boldsymbol{A} = \begin{bmatrix} 1 & \theta_{k-1} & \theta_{k-1}^2 \\ 1 & \theta_k & \theta_k^2 \\ 1 & \theta_{k+1} & \theta_{k+1}^2 \end{bmatrix} \tag{25}$$

and

$$\boldsymbol{x} = \begin{bmatrix} c \\ b \\ a \end{bmatrix}, \quad \boldsymbol{b} = \begin{bmatrix} P(\theta_{k-1}) \\ P(\theta_k) \\ P(\theta_{k+1}) \end{bmatrix} \tag{26}$$

Then

$$\boldsymbol{b} = \boldsymbol{A}\boldsymbol{x} \tag{27}$$

Considering $\boldsymbol{A}$ is a Vandermonde matrix, $\theta_{k+1} \neq \theta_k \neq \theta_{k-1}$, $\det \boldsymbol{A} \neq 0$ and $\boldsymbol{A}$ is invertible, it has a unique inverse matrix, denoted as $\boldsymbol{A}^{-1}$. Then,

$$\boldsymbol{x} = \boldsymbol{A}^{-1}\boldsymbol{b} \tag{28}$$

Since $\boldsymbol{A}$ is a Vandermonde matrix, using Lagrangian interpolation, we directly have equations (29)–(31). And then, we have equation (32).

$$\boldsymbol{A}^{-1} = \begin{bmatrix} \dfrac{(-1)^2\theta_k\theta_{k+1}}{(\theta_{k-1}-\theta_k)(\theta_{k-1}-\theta_{k+1})} & \dfrac{(-1)^2\theta_{k-1}\theta_{k+1}}{(\theta_k-\theta_{k-1})(\theta_k-\theta_{k+1})} & \dfrac{(-1)^2\theta_{k-1}\theta_k}{(\theta_{k+1}-\theta_{k-1})(\theta_{k+1}-\theta_k)} \\ \dfrac{(-1)(\theta_k+\theta_{k+1})}{(\theta_{k-1}-\theta_k)(\theta_{k-1}-\theta_{k+1})} & \dfrac{(-1)(\theta_{k-1}+\theta_{k+1})}{(\theta_k-\theta_{k-1})(\theta_k-\theta_{k+1})} & \dfrac{(-1)(\theta_{k-1}+\theta_k)}{(\theta_{k+1}-\theta_{k-1})(\theta_{k+1}-\theta_k)} \\ \dfrac{1}{(\theta_{k-1}-\theta_k)(\theta_{k-1}-\theta_{k+1})} & \dfrac{1}{(\theta_k-\theta_{k-1})(\theta_k-\theta_{k+1})} & \dfrac{1}{(\theta_{k+1}-\theta_{k-1})(\theta_{k+1}-\theta_k)} \end{bmatrix} \tag{29}$$

$$\begin{aligned}\boldsymbol{b}=&\frac{(-1)(\theta_k+\theta_{k+1})P(\theta_{k-1})}{(\theta_{k-1}-\theta_k)(\theta_{k-1}-\theta_{k+1})}+\frac{(-1)(\theta_{k-1}+\theta_{k+1})P(\theta_k)}{(\theta_k-\theta_{k-1})(\theta_k-\theta_{k+1})}+\frac{(-1)(\theta_{k-1}+\theta_k)P(\theta_{k+1})}{(\theta_{k+1}-\theta_{k-1})(\theta_{k+1}-\theta_k)}\\=&\frac{(\theta_{k-1}^2-\theta_{k+1}^2)P(\theta_k)-(\theta_{k-1}^2-\theta_k^2)P(\theta_{k+1})-(\theta_k^2-\theta_{k+1}^2)P(\theta_{k-1})}{(\theta_{k-1}-\theta_k)(\theta_{k-1}-\theta_{k+1})(\theta_k-\theta_{k+1})}\\=&\frac{(\theta_k^2-\theta_{k+1}^2)(P(\theta_k)-P(\theta_{k-1}))-(\theta_{k-1}^2-\theta_k^2)(P(\theta_k)-P(\theta_{k+1}))}{(\theta_{k-1}-\theta_k)(\theta_{k-1}-\theta_{k+1})(\theta_k-\theta_{k+1})}\end{aligned}\tag{30}$$

$$\begin{aligned}\boldsymbol{a}=&\frac{P(\theta_{k-1})}{(\theta_{k-1}-\theta_k)(\theta_{k-1}-\theta_{k+1})}+\frac{P(\theta_k)}{(\theta_k-\theta_{k-1})(\theta_k-\theta_{k+1})}+\frac{P(\theta_{k+1})}{(\theta_{k+1}-\theta_{k-1})(\theta_{k+1}-\theta_k)}\\=&\frac{(\theta_k-\theta_{k+1})P(\theta_{k-1})-(\theta_{k-1}-\theta_{k+1})P(\theta_k)+(\theta_{k-1}-\theta_k)P(\theta_{k+1})}{(\theta_{k-1}-\theta_k)(\theta_{k-1}-\theta_{k+1})(\theta_k-\theta_{k+1})}\\=&\frac{(\theta_k-\theta_{k-1})(P(\theta_k)-P(\theta_{k+1}))-(\theta_k-\theta_{k+1})(P(\theta_k)-P(\theta_{k-1}))}{(\theta_{k-1}-\theta_k)(\theta_{k-1}-\theta_{k+1})(\theta_k-\theta_{k+1})}\end{aligned}\tag{31}$$

$$\theta_{QI}=-\frac{1}{2}\times\frac{(\theta_k^2-\theta_{k+1}^2)(P(\theta_k)-P(\theta_{k-1}))-(\theta_{k-1}^2-\theta_k^2)(P(\theta_k)-P(\theta_{k+1}))}{(\theta_k-\theta_{k-1})(P(\theta_k)-P(\theta_{k+1}))-(\theta_k-\theta_{k+1})(P(\theta_k)-P(\theta_{k-1}))}\tag{32}$$

3. Proposed Root-MUSIC plus Max-RP-QI

In this section, to achieve the CRLB, Root-MUSIC [30], [31] is combined with the proposed Max-RP-QI to form a blended scheme: Root-MUSIC plus Max-RP-QI as shown in Figure 4. The left part of this array structure uses a small-scale number Q of subarrays, totally $N_a = MQ$ antennas, to generate a set of candidate solutions. For the right part of this HAD structure, the Max-RP-QI is adopted to output the optimal DOA, which is to choose the true DOA value from the set of candidate solutions.

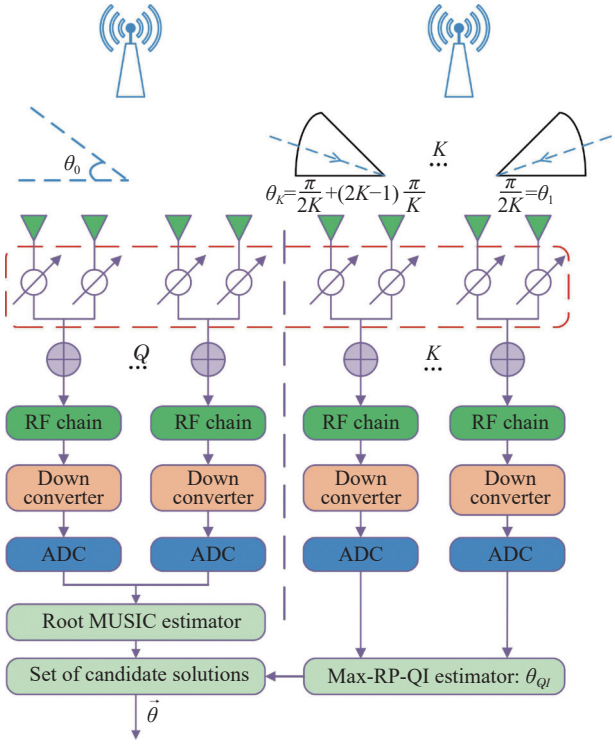

Figure 4 Proposed root-MUSIC plus max-RP-QI structure.

Given the initial phases of all analog phase shifters of the left part in Figure 4 are zeros, we have

$$\boldsymbol{V}_A=\frac{1}{\sqrt{M}}[1,1,\ldots,1]^{\mathrm{T}}\tag{33}$$

According to (33), the receive vector consisting of all outputs of the subarray in the left part is expressed as follows

$$\begin{aligned}\boldsymbol{y}_L(t)&=[y_1(t),\cdots,y_q(t),\cdots,y_Q(t)]^{\mathrm{T}}\\&=\frac{1}{\sqrt{M}}\boldsymbol{a}_Q(\theta_0)g(\theta_0)s(t)+[w_1(t),w_2(t),\ldots,w_Q(t)]^{\mathrm{T}}\end{aligned}\tag{34}$$

where $\boldsymbol{a}_Q(\theta_0)$ is the associated small-scale array manifold written as

$$\boldsymbol{a}_Q(\theta_0)=\left[\mathrm{e}^{\mathrm{j}2\pi\mu_{\theta_0}(1)},\mathrm{e}^{\mathrm{j}2\pi\mu_{\theta_0}(2)},\cdots,\mathrm{e}^{\mathrm{j}2\pi\mu_{\theta_0}(Q-1)}\right]^{\mathrm{T}}\tag{35}$$

where

$$\mu_{\theta_0}(q)=\frac{Md_q\sin\theta_0}{\lambda},q=1,2,\ldots,Q-1\tag{36}$$

And $g(\theta_0)$ in (34) is the constant obtained by summing the elements of each subarray oriented vector can be denoted as

$$g(\theta_0)=\sum_{m=1}^{M}\mathrm{e}^{\mathrm{j}\frac{2\pi}{\lambda}(m-1)d\sin\theta_0}=\frac{1-\mathrm{e}^{\mathrm{j}\frac{2\pi}{\lambda}Md\sin\theta_0}}{1-\mathrm{e}^{\mathrm{j}\frac{2\pi}{\lambda}d\sin\theta_0}}\tag{37}$$

Therefore, the array manifold $\boldsymbol{a}_y(\theta_0)$ is defined as

$$\boldsymbol{a}_y(\theta_0)=\boldsymbol{a}_Q(\theta_0)g(\theta_0)\tag{38}$$

From (34), the covariance matrix of the output vector is defined as

$$\boldsymbol{R}_y = \mathbb{E}[\boldsymbol{y}\boldsymbol{y}^{\mathrm{H}}]^{\mathrm{T}} = \boldsymbol{a}_y \boldsymbol{R}_s \boldsymbol{a}_y^{\mathrm{H}} + \boldsymbol{R}_w \tag{39}$$

Subsitting equations (35) and (37) into (40), the above formula is rewritten as

$$\boldsymbol{R}_y = \frac{1}{M}\sigma_s^2 \|g(\theta_0)\|^2 \boldsymbol{a}_Q(\theta_0)\boldsymbol{a}_Q^{\mathrm{H}}(\theta_0) + \sigma_w^2 \boldsymbol{I} \tag{40}$$

where σ_s^2 represents the variance of the receive signal being the average receive signal power and σ_s^2 stands for the noise variance. Furthermore, similar to the conventional Root-MUSIC method, the eigenvalue decomposition (EVD) of $\boldsymbol{R}_y$ is expressed as

$$\boldsymbol{R}_y = \boldsymbol{U}\Sigma\boldsymbol{U}^{\mathrm{H}} = [\boldsymbol{U}_S\, \boldsymbol{U}_N]\Sigma[\boldsymbol{U}_S\, \boldsymbol{U}_N]^{\mathrm{H}} \tag{41}$$

where

$$\Sigma = \begin{bmatrix} \sigma_s^2 + \sigma_w^2 & 0 & \dots & 0 \\ 0 & \sigma_w^2 & \dots & 0 \\ \vdots & \vdots & \ddots & \vdots \\ 0 & 0 & \dots & \sigma_w^2 \end{bmatrix} \tag{42}$$

is a diagonal matrix with elements being the corresponding eigen-values of $\boldsymbol{R}_y$. And the $Q \times 1$ matrix $\boldsymbol{U}_S$ contains the singular vectors corresponding to the largest eigen-value, the matrix $\boldsymbol{U}_N$ contains the eigen-vectors corresponding to the $Q-1$ smallest singular values. Then, we compute

$$\varphi(\theta) = \frac{1}{\|\boldsymbol{U}_N^{\mathrm{H}}\boldsymbol{a}_y^{\mathrm{H}}\|^2} = \frac{1}{\|g(\theta_0)\|^2 \|\boldsymbol{a}_Q^{\mathrm{H}}\boldsymbol{U}_N\boldsymbol{U}_N^{\mathrm{H}}\boldsymbol{a}_Q\|} \tag{43}$$

which will have peaks at the signal directions.

In order to obtain the peak point of equation (43), the Root-MUSIC algorithm is adopted because it does not require linear search, has low complexity and can obtain approximate analytical solutions. Then, the polynomial $f(z)$ is defined as

$$f(z) = g^{\mathrm{H}}(z)\boldsymbol{a}_Q^{\mathrm{H}}(z)\boldsymbol{U}_N\boldsymbol{U}_N^{\mathrm{H}}\boldsymbol{a}_Q(z)g(z) = 0 \tag{44}$$

where

$$z = \mathrm{e}^{\mathrm{j}\frac{2\pi}{\lambda}Md\sin\theta} \tag{45}$$

Obviously, the order of the polynomial is $2(Q-1)$, which means that the polynomial has $2(Q-1)$ roots. Then, for an equally spaced uniform linear array, the set of the candidate solutions can be given by

$$\Theta_z = \left\{\tilde{\theta}_1, \tilde{\theta}_2, \dots, \tilde{\theta}_{2Q-2}\right\} \tag{46}$$

where

$$\tilde{\theta}_q = \arcsin\left(\frac{\lambda \arg z_q}{2\pi M d}\right) \tag{47}$$

After estimating the DOA value θ_{QI} using the right-hand structure, the optimal solution can be written as

$$\overrightarrow{\theta} = \arg\min_{\theta_q \in \Theta_z} \|\tilde{\theta}_q - \overline{\theta}_{QI}\|^2 \tag{48}$$

This completes the design of the proposed root-MUISC plus max-RP-QI.

4. Complexity analysis

In what follows, we make an analysis of computational complexities of the proposed three estimators with previous TLHAD method as a complexity reference. Thus, the complexity (FLOPs) of Max-RP is as follows:

$$C_{\text{Max-RP}} = O\Big\{K(3ML^2 + L^2 - M)\Big\} \tag{49}$$

The complexity (FLOPs) of Max-RP-QI is

$$\begin{aligned} C_{\text{Max-RP-QI}} =& O\Big\{K(3ML^2 + L^2 - M) \\ &+ \frac{1}{3}K^3 + 2K^2 + \frac{2}{3}K\Big\} \end{aligned} \tag{50}$$

The complexity (FLOPs) of root-MUSIC plus Max-RP-QI is

$$\begin{aligned} &C_{\text{root-MUSICplusMax-RP-QI}} \\ &= O\Big\{(K-2) \times \big((3ML^2 + L^2 - M) \\ &\quad + \frac{1}{3}K^3 + 2K^2 + \frac{2}{3}K\big) + M^3 + 2ML^2\Big\} \end{aligned} \tag{51}$$

And the complexity (FLOPs) of the existing TLHAD is

$$C_{\text{TLHAD}} = O\Big\{M^3 + M^2(2L-1) + \frac{N^3}{4} + \frac{N^2}{4}(2L-1)\Big\} \tag{52}$$

Considering the number of antennas tends to large-scale or ultra-large-scale, compare with the previous TLHAD estimators, the computational complexities of the proposed three estimators are significantly reduced.

IV. Numerical Results

In this section, we present simulation results to the performance of the three estimators: Max-RP, Max-RP-QI and Root-MUSIC Plus Max-RP-QI with the hybrid CRLB as a performance benchmak. Simulation parameters are chosen as shown: the direction of emitter $\theta_0 = 41°$, and $L \in \{50, 100, 200, 400, 800\}$. In large-scale and ultra-large-scale MIMO scenarios, the number of antennas at receive array is set $N = 1024$ and $M = 8$.

Figure 5 demonstrates the receive power versus DOA estimated by Max-RP for $N = 1024$, $K = 128$, and $\theta_0 \in \{41°, 61°\}$. As can be seen, $P(\theta_k)$ is maximized around the source direction θ for three different SNRs (0 dB, 5 dB, 10 dB). And we find that the proposed Max-RP estimators can provide a prefect estimate of direction for SNR $\geq$ 5 dB. This means that when the number of antennas tends to large-scale or ultra-large-scale,

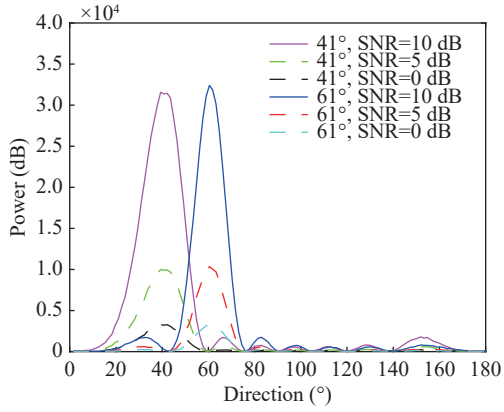

Figure 5 Receive power versus direction estimated by the proposed Max-RP method.

the better estimation performance can be obtained as the number K of subarrays increase.

Figure 6 plots the root mean squared error (RMSE) versus SNR of the proposed three methods, where the corresponding hybrid CRLBs are used as a performance benchmark. From this figure, it is seen that the proposed Root-MUSIC plus Max-RP-QI method can achieve the CRLBs with the SNR $\geq$ 10dB while Max-RP and Max-RP-QI are still substantial gaps from the hybrid CRLBs.

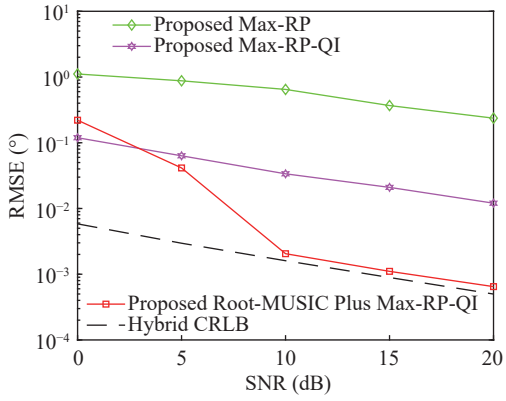

Figure 6 RMSE versus SNR of the proposed methods.

To observe the impact of the different L of number of the snapshots on the proposed schemes, in Figure 7, the value of L is varied from 50 to 800, given the number of antennas $N = 1024$, and the number of sunarray $K = 128$. Thus, Figure 7 plots the RMSE verus the number of snapshots of the proposed method. It can be observed in Figure 7 that the performance of the proposed Root-MUSIC plus Max-RP-QI method accordingly improves as the number L of snapshots/sampling increases. In addition, regardless of the value of the number of snapshots/sampling points, the proposed Root-MUSIC plus Max-RP-QI method always achieves the hybrid CLRB.

To evaluate the impact of the number of assigned subarrays of the left part structure on perfromance, the

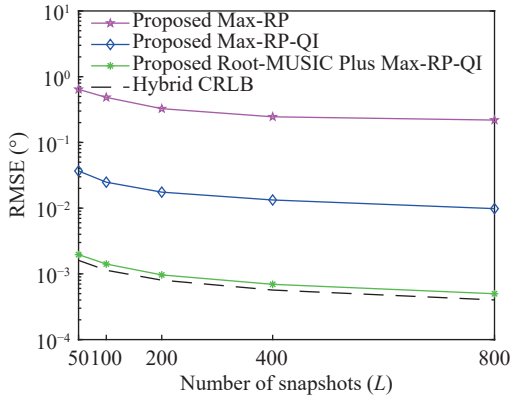

Figure 7 RMSE versus snapshots of the proposed methods.

Figure 8 plots the curves of RMSE versus SNR for K_L=8, 16, and 32, where K_L denotes three different numbers of left-side subarrays for Root-MUSIC. Observing this figure, we find that the proposed Root-MUSIC Plus Max-RP-QI estimator can achieve the hybrid CRLB for $K_L = 32$. It means that the appropriate proportion of left-side subarrays for Root-MUSIC can be chosen in accordance with the performance requirements of different scenarios.

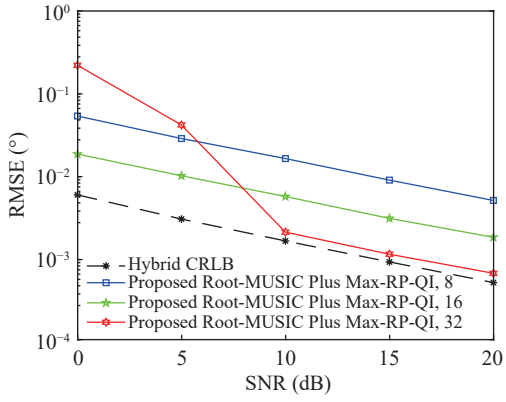

Figure 8 RMSE versus SNR of the proposed Root-MUSIC Plus Max-RP-QI method for different number of subarrays K.

Figure 9 illustrates the curves of complexity versus the number N of antennas with N varying from 1024 to 8192. From Figure 9, it is shown that the proposed three methods have approximately the same computational complexities. And it is seen that as the number of total antennas increases, the complexities of all proposed methods increase much slower than that of the existing TLHAD in [25].

V. Conclusions

In this paper, based on the hybrid massive MIMO receive array structure, the three DOA estimators: Max-RP, Max-RP-QI, and Root-MUSIC Plus Max-RP-QI, were poposed, which succefully eliminate phase ambiguity in a single time-slot. In summary, the proposed methods have an increasing precision order as follows: Max-RP, Max-RP-QI, and Root-MUSIC Plus Max-RP-QI.

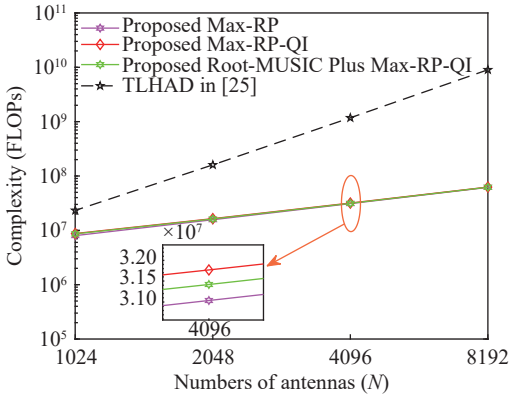

Figure 9 Complexity versus number of antennas of the proposed methods.

Moreover, the proposed Root-MUSIC Plus Max-RP-QI can achieve CRLB with approximately identical computational complexity as the first two methods. This makes them attractive for the future applications of DOA-measurement based sensing in IoT, UAV, satellite communications, WSNs, direction modulation network, and beyond 5G.

Acknowledgement

This work was supported in part by the National Natural Science Foundation of China (Grant Nos. U22A 2002 and 62071234), the Hainan Province Science and Technology Special Fund (Grant No. ZDKJ2021022), and the Scientific Research Fund Project of Hainan University (Grant No. KYQD(ZR)-21008).

References

[1] T. E. Tuncer and B. Friedlander, *Classical and Modern Direction-of-Arrival Estimation*. Academic Press, New York, NY, USA, 2009.

[2] S. A. Zekavat and R. M. Buehrer, *Handbook of Position Location: Theory, Practice, and Advances*, 2nd ed., IEEE Press, Hoboken, NJ, USA, pp. 33 − 34, 2019.

[3] J. H. Zhao, S. J. Ni, L. H. Yang, *et al.*, "Multiband cooperation for 5G HetNets: a promising network paradigm," *IEEE Vehicular Technology Magazine*, vol. 14, no. 4, pp. 85–93, 2019.

[4] J. H. Zhao, J. Liu, L. H. Yang, *et al.*, "Future 5G-oriented system for urban rail transit: opportunities and challenges," *China Communications*, vol. 18, no. 2, pp. 1–12, 2021.

[5] F. Shu, X. M. Wu, J. S. Hu, *et al.*, "Secure and precise wireless transmission for random-subcarrier-selection-based directional modulation transmit antenna array," *IEEE Journal on Selected Areas in Communications*, vol. 36, no. 4, pp. 890–904, 2018.

[6] F. Shu, X. M. Wu, J. Li, *et al.*, "Robust synthesis scheme for secure multi-beam directional modulation in broadcasting systems," *IEEE Access*, vol. 4, pp. 6614–6623, 2016.

[7] R. W. Heath, N. González-Prelcic, S. Rangan, *et al.*, "An overview of signal processing techniques for millimeter wave MIMO systems," *IEEE Journal of Selected Topics in Signal Processing*, vol. 10, no. 3, pp. 436–453, 2016.

[8] J. H. Zhao, L. H. Yang, M. H. Xia, *et al.*, "Unified analysis of coordinated multipoint transmissions in mmWave cellular networks," *IEEE Internet of Things Journal*, vol. 9, no. 14, pp. 12166–12180, 2022.

[9] X. Cheng, W. P. Shi, W. L. Cai, *et al.*, "Communication-efficient coordinated RSS-based distributed passive localization via drone cluster," *IEEE Transactions on Vehicular Technology*, vol. 71, no. 1, pp. 1072–1076, 2022.

[10] C. Li, Y. Xu, J. J. Xia, *et al.*, "Protecting secure communication under UAV smart attack with imperfect channel estimation," *IEEE Access*, vol. 6, pp. 76395–76401, 2018.

[11] Y. W. Li, Z. C. Zhang, L. Wu, *et al.*, "5G communication signal based localization with a single base station," in *2020 IEEE 92nd Vehicular Technology Conference (VTC2020-Fall)*, Victoria, BC, Canada, pp. 1–5, 2020.

[12] Y. Wang and K. C. Ho, "Unified near-field and far-field localization for AOA and hybrid AOA-TDOA positionings," *IEEE Transactions on Wireless Communications*, vol. 17, no. 2, pp. 1242–1254, 2018.

[13] R. Zhang, T. J. Lim, Y. C. Liang, *et al.*, "Multi-antenna based spectrum sensing for cognitive radios: a GLRT approach," *IEEE Transactions on Communications*, vol. 58, no. 1, pp. 84–88, 2010.

[14] Q. J. Jie, X. C. Zhan, F. Shu, *et al.*, "High-performance passive Eigen-model-based detectors of single emitter using massive MIMO receivers," *IEEE Wireless Communications Letters*, vol. 11, no. 4, pp. 836–840, 2022.

[15] Y. F. Li, F. Shu, J. S. Hu, *et al.*, Machine learning methods for inferring the number of UAV emitters via massive MIMO receive array, *arXiv preprint*, arXiv: 2203.00917, 2022.

[16] X. M. Meng and J. Zhu, "A generalized sparse Bayesian learning algorithm for 1-bit DOA estimation," *IEEE Communications Letters*, vol. 22, no. 7, pp. 1414–1417, 2018.

[17] B. H. Shi, N. Chen, X. C. Zhu, *et al.*, "Impact of low-resolution ADC on DOA estimation performance for massive MIMO receive array," *IEEE Systems Journal*, vol. 16, no. 2, pp. 2635–2638, 2022.

[18] B. H. Shi, L. L. Zhu, W. L. Cai, *et al.*, "On performance loss of DOA measurement using massive MIMO receiver with mixed-ADCs," *IEEE Wireless Communications Letters*, vol. 11, no. 8, pp. 1614–1618, 2022.

[19] S. F. Han, I. C. Lin, C. Rowell, *et al.*, "Large scale antenna system with hybrid digital and analog beamforming structure," in *2014 IEEE International Conference on Communications Workshops (ICC)*, Sydney, NSW, Australia, pp. 842–847, 2014.

[20] F. Shu, Y. L. Qin, T. T. Liu, *et al.*, "Low-complexity and high-resolution DOA estimation for hybrid analog and digital massive MIMO receive array," *IEEE Transactions on Communications*, vol. 66, no. 6, pp. 2487–2501, 2018.

[21] R. Y. Zhang, B. Shim, and W. Wu, "Direction-of-arrival estimation for large antenna arrays with hybrid analog and digital architectures," *IEEE Transactions on Signal Processing*, vol. 70, pp. 72–88, 2021.

[22] S. Li, Y. S. Liu, L. You, *et al.*, "Covariance matrix reconstruction for DOA estimation in hybrid massive MIMO systems," *IEEE Wireless Communications Letters*, vol. 9, no. 8, pp. 1196–1200, 2020.

[23] B. H. Shi, X. Y. Jiang, N. Chen, *et al.*, "Fast ambiguous DOA elimination method of DOA measurement for hybrid massive MIMO receiver," *Science China Information Science*, vol. 65, no. 5, article no. 159302, 2022.

[24] H. J. Huang, J. Yang, H. Huang, *et al.*, "Deep learning for super-resolution channel estimation and DOA estimation based massive MIMO system," *IEEE Transactions on Vehicular Technology*, vol. 67, no. 9, pp. 8549–8560, 2018.

[25] F. Shu, Y. W. Chen, X. C. Zhan, *et al.*, Machine-learning-aided massive hybrid analog and digital MIMO DOA estimation for future wireless networks, *arXiv preprint*, arXiv: 2201.04452, 2022.

[26] B. B. Li, X. F. Zhang, J. F. Li, *et al.*, "DOA estimation of non-circular source for large uniform linear array with a single snapshot: extended DFT method," *IEEE Communications Letters*, vol. 25, no. 12, pp. 3843–3847, 2021.
[27] D. Hu, Y. H. Zhang, L. H. He, *et al.*, "Low-complexity deep-learning-based DOA estimation for hybrid massive MIMO systems with uniform circular arrays," *IEEE Wireless Communications Letters*, vol. 9, no. 1, pp. 83–86, 2020.
[28] Z. H. Zhuang, L. Xu, J. Y. Li, *et al.*, "Machine-learning-based high-resolution DOA measurement and robust directional modulation for hybrid analog-digital massive MIMO transceiver," *Science China Information Sciences*, vol. 63, no. 8, article no. 180302, 2020.
[29] R. A. Horn and C. R. Johnson, *Matrix Analysis*, 2nd ed., Cambridge University Press, New York, NY, USA, 2013.
[30] B. D. Rao and K. V. S. Hari, "Performance analysis of Root-Music," *IEEE Transactions on Acoustics, Speech, and Signal Processing*, vol. 37, no. 12, pp. 1939–1949, 1989.
[31] B. Friedlander, "The root-MUSIC algorithm for direction finding with interpolated arrays," *Signal Processing*, vol. 30, no. 1, pp. 15–29, 1993.

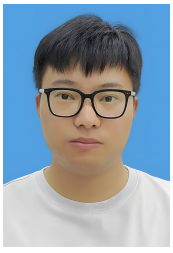

Xichao ZHAN was born in Anhui Province, China. He is a postgraduate student in the School of Information and Communication Engineer at Hainan University, Haikou, China. His research interest is DOA estimation.
(Email: zhange0223@163.com)

Zhongwen SUN was born in Shandong Province, China. He is a postgraduate student in the School of Information and Communication Engineer at Hainan University, Haikou, China. His research interests include channel estimation and wireless communication.
(Email: yukisoranya@gmail.com)

Feng SHU is a Professor with the School of Information and Communication Engineer at Hainan University, Haikou, China. His research interests include massive MIMO (especially directional and spatial modulations), DOA measurements, wireless location, and machine learning for mobile communications. In 2020, he was awarded with the Leading Talents of Hainan Province. Also, he has been awarded with Ming Jian Scholar Chair Professor and Fujian Hundred-talents Program in Fujian Province, China. He has published more 200 journal papers and with more than 150 SCI-indexed papers and more than 100 IEEE journal papers. Now, he serves as an Editor for IEEE journals *IEEE Systems Journal* and *IEEE Wireless Communications Letters*.
(Email: shufeng0101@163.com)

Yiwen CHEN was born in Henan Province, China. He is a postgraduate student in the School of Information and Communication Engineer at Hainan University, Haikou, China. His research interests include emitter detection and DOA estimation.
(Email: cyw1978650281@163.com)

Xin CHENG received the B.S. degrees from the Nanjing University of Science and Technology, China, in 2018, where he is currently pursuing the Ph.D. degree with the School of Electronic and Optical Engineering. His research interests include wireless communication, signal processing, and distributed computation. (Email: 118104010558@njust.edu.cn)

Yuanyuan WU is a Professor at the School of Information and Communication Engineering, Hainan University, Haikou, China. Her research interests include control automation, digital image processing, multi-source information fusion, and artificial intelligence.
(Email: wyuanyuan@163.com)

Qi ZHANG received the M.S. degree in electronic and communication engineering from Hainan University, in 2021. He is currently pursuing the Ph.D. degree with the School of Information and Communication Engineering at Hainan University. His research interests include wireless physical-layer security, signal processing and covert communication.
(Email: hdzhangqi0509@163.com)

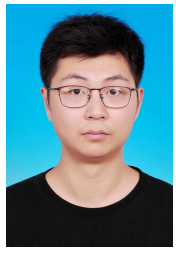

Yifan LI is a Ph.D student with the School of Electronic and Optical Engineering at Nanjing University of Science and Technology, Nanjing, China. His research interests include localization, array processing and machine learning.
(Email: liyifan97@foxmail.com)

Peng ZHANG is a postgraduate student in the School of Information and Communication Engineer at Hainan University, Haikou, China. His research interests include IRS-aided relay systems.
(Email:15670952773@163.com)